into acetate buffer (10 mM, pH* 6.1, in D_2O) for variable time periods before being pulse-labeled (acetate-Mes-tris; I = 0.2 M, pH* 10.2, in D_2O); the final pH* was 10.2. The final pH* of all steps was checked in independent experiments. Labeling was quenched after 20 ms by dilution into buffer (acetate-Mes-tris; I = 0.25 M, pH* 1.9, in D_2O) to final pH* 5.6. This solution was injected into a reservoir that contained a 1.1 molar excess of bovine hemin (Sigma) to apoprotein.

20. Reconstituted protein was concentrated (Amicon) to ~2 ml, equilibrated with CO and reduced with sodium dithionite. Sodium dithionite was removed by successive cycles of concentration and redilution in CO-equilibrated potassium phosphate buffer (50 mM) in an Amicon concentrator. The protein was concentrated to 3 to 4 mM and equilibrated for 12 hours at 4°C and 4 hours at 35°C before the data were collected.
21. Double quantum and NOESY spectra were collected for each sample on a 600-MHz Bruker AMX spectrometer. A total of 32 transients of 4095 (2Q) or 8192 (NOESY) real data points were recorded for each of 512 t_1 increments. Data were processed with zero filling to 4K complex points and sine bell multiplication in both dimensions with the FTNMR program (Hare Research, Woodinville, WA). Data at each time point were normalized to three nonexchangeable protons and to control experiments in which fully folded or fully unfolded protein was exposed to the labeling pulse (*18*).
22. A. A. Schreier and R. L. Baldwin, *J. Mol. Biol.* **105**, 409 (1976).
23. S. W. Englander and L. Mayne, *Annu. Rev. Biophys. Biomol. Struct.* **21**, 243 (1992).
24. G. A. Elove and H. Roder, *Protein Refolding* (American Chemical Society, Washington, DC, 1991), pp. 51–63.
25. Changing the pH or the duration of the labeling pulse may discriminate between a sequential and a parallel folding pathway (*17, 23, 24*). Experiments were carried out in which the length of the labeling pulse was varied after a fixed (10.2 ms) folding time. The proton occupancies remained constant when the labeling pulse was lengthened (two to three times longer). Variation of the pulse pH is not feasible for apoMb due to the instability of the apoprotein at pH >10.2, and the tendency to aggregate at pH <9.5.
26. D. Barrick and R. L. Baldwin, *Biochemistry* **32**, 3790 (1993).
27. T. E. Creighton, *Curr. Biol.* **1**, 8 (1991).
28. R. L. Baldwin and H. Roder, *ibid.*, p. 218.
29. J. P. Waltho, V. A. Feher, G. Merutka, H. J. Dyson, P. E. Wright, *Biochemistry* **32**, 6337 (1993); H.-C. Shin *et al.*, *ibid.*, p. 6356.
30. O. B. Ptitsyn and A. A. Rashin, *Biophys. Chem.* **3**, 1 (1975); T. J. Richmond and F. M. Richards, *J. Mol. Biol.* **119**, 537 (1978); F. E. Cohen, T. J. Richmond, F. M. Richards, *ibid.* **132**, 275 (1979); F. E. Cohen, M. J. E. Sternberg, D. C. Phillips, *Nature* **286**, 632 (1980); M. Gerritsen, K.-C. Chou, G. Nemethy, H. A. Scheraga, *Biopolymers* **24**, 1271 (1985); D. Bashford, F. E. Cohen, M. Karplus, I. D. Kuntz, D. L. Weaver, *Proteins Struct. Funct. Genet.* **4**, 211 (1988); G. Chelvanayagam, Z. Reich, R. Bringas, P. Argos, *J. Mol. Biol.* **227**, 901 (1992).
31. J. B. Udgaonkar and R. L. Baldwin, *Proc. Natl. Acad. Sci. U.S.A.* **87**, 8197 (1990); M. Bycroft, A. Matouschek, J. T. Kellis Jr., L. Serrano, A. R. Fersht, *Nature* **346**, 488 (1990); A. Matouscheck, J. T. Kellis Jr., L. Serrano, M. Bycroft, A. R. Fersht, *ibid.*, p. 440; M. S. Briggs and H. Roder, *Proc. Natl. Acad. Sci. U.S.A.* **89**, 2017 (1992); J. Lu and F. W. Dahlquist, *Biochemistry* **31**, 4749 (1992).
32. G. A. Elove, A. F. Chaffotte, H. Roder, M. E. Goldberg, *Biochemistry* **31**, 6876 (1992); S. E. Radford, C. M. Dobson, P. A. Evans, *Nature* **358**, 302 (1992); P. Varley *et al.*, *Science* **260**, 1110 (1993). These papers also report formation of burst phase intermediates observed by stopped-flow CD but, in contrast to that formed by apoMb, these intermediates do not protect amide protons from exchange.
33. In stopped-flow CD experiments (Aviv 62DS Circular Dichroism Spectrometer equipped with a Biologic SFM-3 stopped-flow system), apoMb was unfolded in 6 M urea at pH 6.1 and refolded by dilution (1:7.50) into acetate buffer (10 mM, pH 6.1).
34. X. Cheng and B. P. Schoenborn, *J. Mol. Biol.* **220**, 381 (1991).
35. Supported by NIH grant DK-34909 (P.E.W.) and NIH postdoctoral award GM14541 (P.A.J.). We thank C. R. Matthews for the use of the stopped-flow CD spectrometer (supported by BRS Shared Instrument Grant RR04953 from the National Institutes of Health), H. J. Dyson for discussions and for review of the manuscript, L. Tennant for technical assistance, and D. Barrick, M. Cocco, G. Elöve, F. Hughson, B. Jones, C. Mann, D. Morikis, and Y. Theriault for discussions.

20 April 1993; accepted 23 August 1993

Detection of Transient Protein Folding Populations by Mass Spectrometry

Andrew Miranker, Carol V. Robinson, Sheena E. Radford, Robin T. Aplin, Christopher M. Dobson

Hydrogen-deuterium exchange measurements are becoming increasingly important in studies of the dynamics of protein molecules and, particularly, of their folding behavior. Electrospray ionization mass spectrometry (ESI-MS) has been used to obtain the distribution of masses within a population of protein molecules that had undergone hydrogen exchange in solution. This information is complementary to that from nuclear magnetic resonance spectroscopy (NMR) experiments, which measure the average occupancy of individual sites over the distribution of protein molecules. In experiments with hen lysozyme, a combination of ESI-MS and NMR was used to distinguish between alternative mechanisms of hydrogen exchange, providing insight into the nature and populations of transient folding intermediates. These results have helped to detail the pathways available to a protein during refolding.

Measurements of hydrogen-deuterium exchange have provided considerable insight into protein and peptide stability, protein dynamics including local fluctuations, antibody epitope mapping, allosteric interactions, and protein folding (*1, 2*). The advent of ESI-MS has enabled the determination of accurate molecular weights of picomolar quantities of proteins, typically to within 1 dalton for proteins with molecular weights up to about 20,000 (*3*). This level of accuracy and the ability to observe intact protein molecules have made the observation of hydrogen exchange of proteins by electrospray ionization feasible (*4*). In this report, we show that a combination of ESI-MS and NMR can provide crucial information on the nature and populations of species on the folding pathway of a protein, information that hitherto was not possible to obtain with either technique in isolation.

Experiments were performed with hen egg-white lysozyme, the native structure of which has been characterized in great detail by a variety of experimental and theoretical methods (*5, 6*). The refolding kinetics of this enzyme have been extensively studied under equilibrium conditions in which a cooperative two-state model is well established (*7*). Furthermore, non-equilibrium refolding studies of lysozyme by pulsed hydrogen-exchange labeling and two-dimensional (2D) NMR have already revealed many details of the folding process (*8*). These details include the observation that the two structural lobes of the native protein are also distinct folding domains and that one, the predominantly α helical domain, folds more rapidly than the other, largely a β sheet domain, in the majority of molecules.

A comparison of the ESI-MS spectra of protonated lysozyme and a sample in which all labile hydrogens had been exchanged for deuterium [deuterated lysozyme (*9*)] is shown in Fig. 1. Although both samples had been dissolved in protonated solvent before the spectra were run, the deuterated protein shows an increase in mass of about 80 daltons (*10*). Because lysozyme contains approximately 250 exchangeable hydrogens, these 80 sites represent hydrogens protected from exchange by the compact structure of the native protein under these conditions. Studies with NMR have shown that the majority of these protected hydrogens arise from backbone amide groups (*6, 11*).

Although amide hydrogen exchange can be measured in a consistent manner by ESI-MS and NMR, the nature of these two methods is complementary. The NMR method monitors the average exchange at individual sites, permitting interpretation

A. Miranker, S. E. Radford, C. M. Dobson, Oxford Centre for Molecular Sciences and New Chemistry Laboratory, Oxford University, South Parks Road, Oxford OX1 3QT, United Kingdom.
C. V. Robinson and R. T. Aplin, Oxford Centre for Molecular Sciences and Dyson Perrins Laboratory, Oxford University, South Parks Road, Oxford OX1 3QY, United Kingdom.

of the measured proton occupancies in the context of the native 3D structure. By contrast, it is not possible through ESI-MS to monitor exchange in a residue-specific manner, but different populations of protein molecules with distinct masses can be distinguished. For example, consider the simple case of distinguishing between two distinct dynamic mechanisms, one in which the amides have exchanged completely in 50% of the protein molecules and not at all in the other 50% (Fig. 2A), and a second in which all amides in a protein have exchanged with a probability of 50% (Fig. 2B). These two events produce indistinguishable NMR spectra because the average proton occupancy (50%) is the same over all protein molecules. By contrast, ESI-MS can clearly distinguish between these two mechanisms, because the populations arising from the first mechanism would be seen as two peaks with masses equivalent to the fully deuterated and fully protonated forms, respectively, but the second would result in a unified population with mass equivalent to 50% of the maximum deuterium content. More generally, in light of the large number of amides in protein molecules and the diversity of protein motions that can mediate exchange, a range of possible masses will result. Thus, not only is the mass of a peak informative, but so are its shape and width.

We have used ESI-MS to explore the equilibrium folding behavior of lysozyme under conditions identical to those used in a detailed NMR investigation of the hydrogen exchange rates of individual amides (*11*). Under these conditions (pH 3.8, 69°C), the native protein is in steady state with its denatured forms. Exchange is assumed to occur only in the unfolded protein, which is present as 10 ± 5% of the total protein concentration. If interconversion between the native and denatured states is rapid compared with the exchange rates of amides in the denatured state, then the proton occupancy at a given amide site is uniform over all the protein population. Its magnitude is determined by the exchange rate from the denatured state and the fraction of the time that the protein has spent in that state. This second-order reaction mechanism (EX2) (*12*) is the case for the majority of proteins under most conditions and would yield a single peak in the mass spectrum, diminishing in mass over time (for the exchange of a deuterated protein dissolved in H_2O). On the other hand, if interconversion between native and denatured states is slow with respect to the rate of amide exchange, the exchange reaction is first-order (EX1) and would produce two peaks in the mass spectrum corresponding to the fully exchanged and fully protected forms, respectively. In this case, the intensity of the two peaks and not their masses would change with time. These two mechanisms can be distinguished with NMR by examination of the pH dependence of exchange (*13*). However, this approach can only distinguish between the extremes of these mechanisms and relies on the assumption that the protein motions that facilitate exchange are pH-insensitive.

Exchange was initiated by the dilution of deuterated protein into protonated buffer at pH 3.8 and 69°C. The results (Fig. 3A) show a steady decrease of the total mass with increasing incubation times, with a concomitant narrowing of the distribution of masses. The predominant mechanism of exchange in the experiment is, therefore, EX2. A more detailed analysis can be made by comparison of the observed mass distributions at a time (30 s) when about 50% of the total exchange is complete, with a simulation based on the assumption that

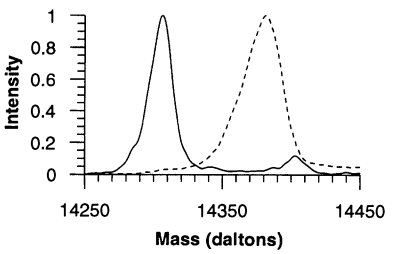

Fig. 1. Traces indicating the ESI-MS spectra (*10*) of lysozyme (solid trace) and deuterated lysozyme (*9*) (dashed trace) freshly dissolved in 80% H_2O and 20% CH_3CN (pH 3.8). Experiments based on near-ultraviolet circular dichroism have shown that the presence of 20% (v/v) CH_3CN does not have a major effect on the native structure of the enzyme under these conditions.

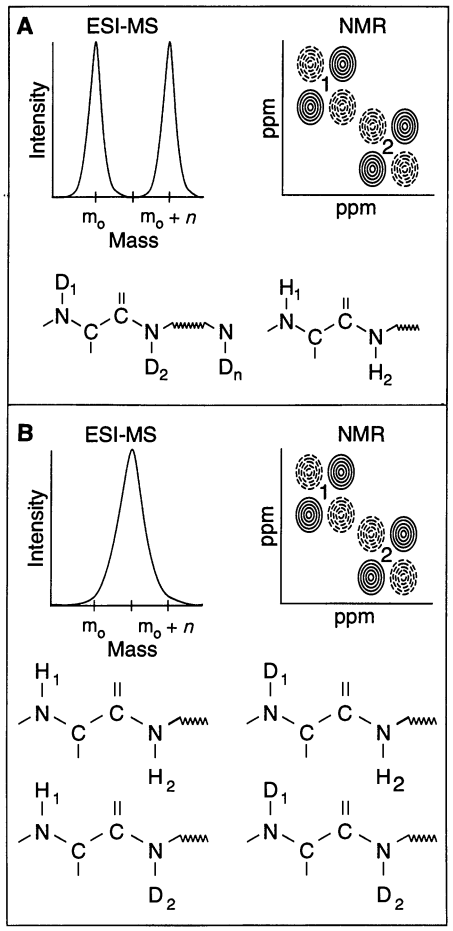

Fig. 2. Schematic of two manifestations of 50% exchange for a collection of *n* amides. In the first case (**A**), 50% of the protein molecules are 100% deuterium for the *n* amides, whereas in the other 50%, the molecules are 100% hydrogen. In the second case (**B**), all amides have a 50% probability of being deuterated. Both (A) and (B) produce identical 2D ^1H NMR spectra, but produce distinct ESI-MS spectra.

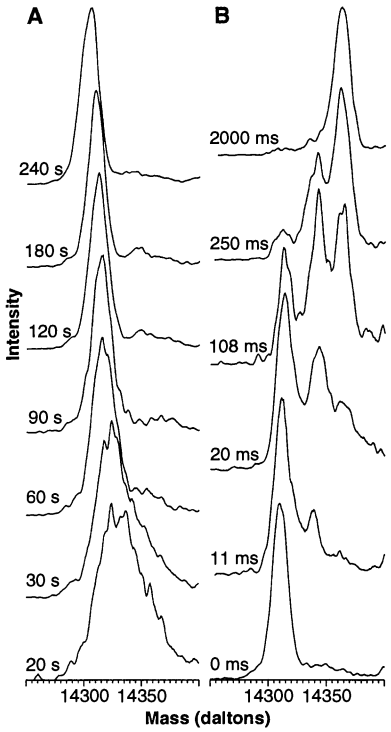

Fig. 3. Time evolution of the ESI-MS spectra (*10*) of (**A**) lysozyme monitoring exchange at pH 3.8, 69°C, and from (**B**) pulse-labeling studies of protein refolding. For (A), deuterated lysozyme was dissolved at 20 mg ml^{-1} in D_2O and equilibrated in a water bath at 69°C. A portion (1 ml) of this solution was then diluted 20-fold into 200 mM sodium acetate buffer in H_2O (pH 3.8, 69°C). After specified lengths of time, hydrogen exchange was quenched by the rapid cooling of the samples (0.5 ml) in thin-walled glass vials in an ice-water bath. Samples were then washed 10 times with 1.0 ml of H_2O (pH 3.8, 4°C) by ultrafiltration to remove residual salts. For (B), the samples were prepared exactly as described in previous pulse-labeling experiments (*8*), except that buffer exchange was made into H_2O (pH 3.8) [as in (A)] and was performed before the samples were sprayed into the mass spectrometer.

exchange occurs solely by an EX2 mechanism (Fig. 4). The presence of a significant proportion of protein molecules with masses greater than or less than that predicted by the simulation reflects the inadequacy of an EX2 mechanism to describe the data. This result was not unexpected, however, because the rate constants for folding ($k = 0.8 \pm 0.5\ s^{-1}$), unfolding ($k = 0.08 \pm 0.04\ s^{-1}$), and exchange from the denatured state ($\bar{k} = 0.19\ s^{-1}$) measured by NMR (*11*) are of similar magnitudes. Indeed, the species with lower or higher masses presumably arise from contributions to the exchange by an EX1 regime, although other mechanisms might also make contributions to exchange. This indicates that ESI-MS should contribute significantly to an understanding of the underlying mechanisms of hydrogen exchange in proteins that are still a topic of debate (*14, 15*).

In a second example, the non-equilibrium refolding of lysozyme was investigated by ESI-MS. In this experiment, a pulse-labeling procedure was performed in which deuterated protein is exposed to a high-pH–labeling pulse at various time points after refolding has been initiated (*16, 17*). Samples were prepared under conditions identical to those in which amide hydrogen protection kinetics were measured by 2D ^1H NMR methods (*8*). Although small variations in the masses and peak widths occur over the time course of the experiment, three distinct species can be detected (Fig. 3B). One of them, at 14,313 daltons, corresponds to the unprotected enzyme and is denoted P0 (*18*). Another peak, at 14,363 daltons, corresponds to the fully protected state. The difference in mass (50 daltons) between P0 and the fully protected peak (P50) is close to the expected protection of the native protein under these conditions. A third peak, however, is also evident in the spectra. This peak, at 14,341 daltons, corresponds to 28 protected amides, a number intermediate between that of the unprotected and the fully protected states.

To identify the nature of this intermediate species and to interpret the kinetics evident in Fig. 3B, the ESI-MS data have been analyzed in light of the refolding protection kinetics observed by NMR. A notable feature of the protection kinetics for lysozyme is that the two structural lobes, which form the active site at their interface, act as distinct folding domains (*19*). Each domain also has biphasic protection kinetics. The fast phase has a time constant (τ) of 5 to 10 ms for each domain and average magnitudes of 40% for the α domain and 25% for the β domain. The slow phases have average magnitudes of 45% and 55% and time constants of 65 ms and 350 ms for the α and β domains, respectively (*20*). The remaining molecules fold on a much longer time scale ($\tau = 16$ s), presumably as a consequence of a third phase associated with *cis-trans* proline isomerization (*21*); this additional phase accounts for the presence of a small proportion (<20%) of molecules unprotected even at the longest refolding times studied. One possible model for folding (model 1) is that the α and β domains fold independently in the fast phase to form two partially folded intermediates, one of which protects only the α domain and one that protects only the β domain. In this model, two populations of intermediates exist at the end of the fast phase. Protection of the α and β domains is then completed with 350-ms and 65-ms time constants, respectively. A second possibility (model 2) is that cooperative folding of α and β domains occurs in the fast phase, resulting in a native-like pattern of protection. The remaining molecules fold by a pathway in which the fully protected state is formed by the sequential protection of first the α and then the β domains. These two models are not distinguished by NMR but can be differentiated by ESI-MS.

The ESI-MS method measures populations of protein molecules distinguished by different numbers of protected amides. This method, therefore, has the unique property of permitting direct observation of P0. Examination of the rate of loss of this peak is informative because P0 makes a significant contribution to the spectra until about 250 ms after the initiation of refolding (Fig. 5); at longer times the residual intensity of P0 can be accounted for by the presence of the very slow folding molecules. This behavior is consistent with both folding models but indicates that a significant proportion of P0 disappears with a time constant that is much longer than the fast protection rates observed by NMR (τ = 5 to 10 ms). Because the results of the pulse-labeling NMR experiments have shown that every amide has a fast protection rate, the results of the present study suggest that the refolding of lysozyme branches into parallel paths before any measurable protection takes place. This indicates that populations of early intermediates are formed that are not significantly protected from exchange.

The number of protected deuterons in peak P28 corresponds closely to the 29 amides that are protected in the α domain in the native state under these conditions. In addition, the difference of 22 daltons between P28 and P50 corresponds reason-

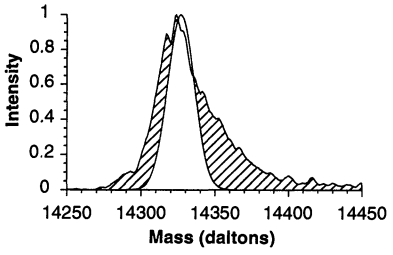

Fig. 4. Traces indicating the ESI-MS spectrum (hatched area) of lysozyme (pH 3.8, 69°C) in which hydrogen exchange has taken place under conditions in which the native and denatured states of the protein are in equilibrium. After 30 s (in Fig. 3A), about 50% of the total exchange had taken place. This spectrum (hatched area) is compared with a simulation of the mass spectrum in which the refolding equilibrium is assumed to contain 10% denatured protein, with exchange occurring by an exclusively EX2 mechanism (unmarked area). The probability of exchange at time t for a given amide of a given protein molecule under EX2 conditions was taken as $e^{-k\lambda t}$, where λ is the fraction of denatured protein (10%) and k is the rate of hydrogen exchange of 46 individual amides in the denatured state of lysozyme determined by NMR (*11*). The distribution of exchange at different times was determined by random sampling of amides from individual protein molecules. Protein molecules were repeatedly sampled until the distribution of exchange converged (26,000 samples). Simulation of the mass spectrum was then achieved by the convolution of the exchange distribution with a Gaussian with the same mean (14,305 daltons) and width at half maximum (20 daltons) as the ESI-MS spectrum of lysozyme in H_2O solution. The measured and simulated time points shown (30 s and 50 s, respectively) were chosen to reflect approximately 50% of the total exchange; the apparent difference in time can be attributed at least in part to error in the measurement of the equilibrium constant, which is very sensitive to small changes in temperature.

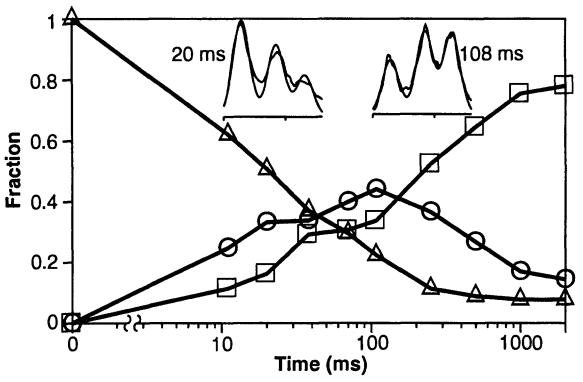

Fig. 5. Time course of the population of the three principal states (triangles, P0; circles, P28; squares, P50) observed in the non-equilibrium refolding of hen lysozyme (Fig. 3B). Sample fits (*18*) are illustrated as insets for t = 20 ms and t = 108 ms. Although fits were made to the raw data, they are illustrated here with respect to the smoothed data shown in Fig. 3B.

ably closely to the 18 amides protected by the β domain in the native enzyme under these conditions. The peak, P28, reaches a maximum intensity at a refolding time of about 100 ms (Fig. 5), consistent with the full protection of the α domain. Reduction in the intensity of this peak to less than 10% of the total does not occur until about 1000 ms, which is consistent with the slow phase of protection of amides in the β domain. Taken together, the data suggest that peak P28 can be assigned to a species in which the α, but not the β, domain is protected from exchange. The resolved nature of this peak and the lack of significant variation in its mass over the time of refolding indicate that it is a well-defined intermediate in the refolding reaction.

The identification of this intermediate allows us to use the kinetics of its formation to distinguish between the two distinct models for folding. Folding model 1 is inconsistent with the rate of formation of P28 because it predicts that 40% of molecules form a state in which only the α domain is protected with a time constant of 5 to 10 ms. By contrast, folding model 2 partitions the fast protection phase of the α domain in two; about 25% of the molecules protect both α and β domains cooperatively, and about 15% of the molecules protect only the α domain. The second model, therefore, predicts population of the intermediate P28 in about 15% of the molecules on this time scale. This rate is more consistent with the observed experimental data (Fig. 5). This conclusion is supported by the kinetics of the formation of the peak, P50. This peak is visible as about 17% of the total protein intensity after a refolding time of only 20 ms. This is not anticipated for folding model 1, which assumes that folding of the α and β domains are independent events in the fast kinetic phase. By contrast, model 2 predicts that a fraction of the protein forms a state with a native-like pattern of protection with a time constant of 5 to 10 ms. The maximum possible magnitude of this phase measured by NMR is about 25%, which is in reasonable agreement with the ESI-MS data given here. In the remainder of molecules, the β domain forms after the α domain, giving rise to the slow phase for the evolution of P50 that is consistent with the 350-ms time constant measured in the NMR experiments.

For two sets of conditions in which the dynamic behavior of lysozyme is different (equilibrium and non-equilibrium refolding), ESI-MS has produced dramatic results. In the case of equilibrium refolding, the ESI-MS data accurately reflect the competitive nature between the refolding and exchange processes and enable the mechanism of exchange to be investigated. For non-equilibrium refolding, a peak is resolved that, by comparison with previously published NMR data (*8*), can be identified as arising from a species with protection only in the α domain. This finding confirms the existence of this species as a well-defined transient intermediate that folds cooperatively. Analysis of the ESI-MS spectra in light of the NMR protection kinetics has enabled us to distinguish between possible dominant pathways sampled in the refolding process. An analysis fully consistent in a quantitative manner with the NMR and ESI-MS kinetics will undoubtedly be more complicated than that presented here. It seems clear, however, from the present data that the dominant pathways sampled in the refolding of lysozyme will more closely resemble folding model 2 than folding model 1.

In a separate study, the development of inhibitor binding activity during refolding was measured by stopped-flow fluorescence and was found to occur with a time constant of about 350 ms, with no evidence for a significant 10-ms kinetic event (*22*). This result suggests that the fast-forming fraction of the population at P50, although having a native-like pattern of protection, is a second intermediate species and not the native state itself. Thus, although the individual domains have folded to native-like states in this intermediate, tertiary interactions spanning the two domains and forming the active-site cleft are lacking. This observation highlights the necessary distinction between states exhibiting native-like patterns of protection and the native 3D structure and underscores the need to study protein refolding by a variety of methods. The rapid developments taking place in mass spectrometry (*23*, *24*) indicate that this technique will play an increasingly important role in these studies.

REFERENCES AND NOTES

1. For reviews, see H. Roder, *Methods Enzymol.* **176**, 446 (1989); R. L. Baldwin, *Curr. Opin. Struct. Biol.* **3**, 84 (1993).
2. Y.-P. Zhang, R. N. A. H. Lewis, R. S. Hodges, R. N. McElhaney, *Biochemistry* **31**, 11572 (1992); F. X. Schmid and R. L. Baldwin, *J. Mol. Biol.* **135**, 199 (1979); M.-F. Jeng and S. W. Englander, *ibid.* **221**, 1045 (1991); A. A. Kossikoff, *Biochemistry* **30**, 1211 (1991); P. S. Kim and R. L. Baldwin, *Annu. Rev. Biochem.* **59**, 631 (1990), and references therein.
3. B. T. Chait and S. B. H. Kent, *Science* **257**, 1885 (1992).
4. V. Katta and B. T. Chait, *Rapid Commun. Mass Spectrom.* **5**, 214 (1991).
5. L. J. Smith, M. J. Sutcliffe, C. Redfield, C. M. Dobson, *J. Mol. Biol.* **229**, 930 (1993); T. G. Pedersen *et al.*, *ibid.* **218**, 413 (1991); J. A. McCammon, B. R. Gelin, M. Karplus, P. G. Wolynes, *Nature* **262**, 325 (1976); C. B. Post, C. M. Dobson, M. Karplus, *Proteins* **5**, 337 (1989).
6. T. Imoto, L. N. Johnson, A. C. T. North, D. C. Phillips, J. A. Rupley, in *The Enzymes*, P. D. Boyer, Ed. (Academic Press, New York, ed. 3, 1972), vol. 7, p. 665.
7. C. Tanford, *Adv. Protein Chem.* **24**, 1 (1970); C. M. Dobson and P. A. Evans, *Biochemistry* **23**, 4267 (1984).
8. S. E. Radford, C. M. Dobson, P. A. Evans, *Nature* **358**, 302 (1992).
9. Deuterated hen egg-white lysozyme was prepared by incubation of lysozyme in D_2O (pH 3.8, 80°C) for 10 min. The protein was then lyophilized. This procedure was repeated three times to ensure complete deuteration of all labile hydrogens.
10. All mass spectra were obtained on a VG Biotech (Cheshire, UK) BioQ triple quadrupole atmospheric pressure mass spectrometer equipped with an electrospray interface. Samples (10 μl) were injected into the electrospray source as a solution (25 pmol μl^{-1}) in water-acetonitrile (4:1) at pH 3.8. Reproducible results were obtained by equilibration of the electrospray interface overnight with the water acetonitrile solution. Unless otherwise stated, all spectra shown are the +11 charge state expressed on a mass scale. The scan range included other charge states to confirm that the reported features are independent of charge state. Each mass spectrum was obtained at least in duplicate, and samples were prepared a minimum of three times.
11. S. E. Radford, M. Buck, K. D. Topping, C. M. Dobson, P. A. Evans, *Proteins* **14**, 237 (1992).
12. A. A. Hvidt and S. O. Nielsen, *Adv. Protein Chem.* **21**, 287 (1966).
13. S. I. Segawa, M. Nakayama, M. Sakane, *Biopolymers* **20**, 1691 (1981); M. Delepierre *et al.*, *J. Mol. Biol.* **197**, 111 (1987).
14. S. W. Englander and L. Mayne, *Annu. Rev. Biophys. Biomol. Struct.* **21**, 243 (1992).
15. C. Woodward, I. Simon, E. Tüchsen, *Mol. Cell. Biochem.* **48**, 135 (1982).
16. J. B. Udgaonkar and R. L. Baldwin, *Nature* **335**, 694 (1988); H. Roder, G. A. Elöve, S. W. Englander, *ibid.*, p. 700.
17. M. Bycroft, A. Matouscheck, J. T. Kellis Jr., L. Serrano, A. R. Fersht, *ibid.* **340**, 488 (1990); J. Lu and F. W. Dahlquist, *Biochemistry* **31**, 4749 (1992); M. S. Briggs and H. Roder, *Proc. Natl. Acad. Sci. U.S.A.* **89**, 2017 (1992).
18. Quantitation of the ESI-MS spectra was performed by nonlinear least squares fitting of Gaussian distributions with a fixed standard deviation and a variable mean and coefficients to resolved peaks in the spectra. The standard deviation was determined from the average width at half maximum (17 daltons) from the t = 0 ms and t = 2000 ms spectra. The coefficient weighted average mass for the three recurring peaks shown in Fig. 3B was 14,313, 14,341, and 14,363 daltons, respectively. The first peak is assumed to be unprotected (P0), and the degree of protection for heavier peaks (P28 and P50) was determined by their difference from the P0 mass. Absolute masses cannot generally be determined accurately from a single charge state. However, the relative mass of these three peaks varied by less than 1 dalton, as compared with a different charge state within the same spectrum and as compared with the same charge state from a repeat experiment. The sum of the coefficients for the fits was normalized to one, and all quoted coefficients represent the average of two experiments. The mass of the unprotected species of 14,313 daltons is slightly larger than that expected for protonated lysozyme (14,305 daltons). This difference can be attributed at least in part to the presence of residual deuterons in the labeling pulse, although the possibility that early intermediates are marginally protected cannot be discounted.
19. A. Miranker, S. E. Radford, M. Karplus, C. M. Dobson, *Nature* **349**, 633 (1991).
20. Magnitudes and time constants were averaged from table 1 of (*8*). Residues 8-36, -63, -64, -78, and 92-125 were ascribed to the α helical domain, with all others ascribed to the β sheet domain. Magnitudes are expressed to the nearest 5%, and time constants are expressed to the nearest 5 ms and 50 ms for time constants less than and greater than 100 ms, respectively. Residue 27 was not included in the averages.

21. S. Kato, N. Shimamoto, H. Utiyama, *Biochemistry* **21**, 38 (1982).
22. L. Itzhaki, S. E. Radford, C. M. Dobson, P. A. Evans, unpublished data.
23. B. S. Larsen and C. N. McEwen, *Rapid Commun. Mass Spectrom.* **6**, 172 (1992); D. Suckau *et al.*, *Proc. Natl. Acad. Sci. U.S.A.* **90**, 790 (1993).
24. In a recent paper, the use of fast-atom–bombardment mass spectrometry in conjunction with protein proteolysis indicated the feasibility of detecting hydrogen exchange within segments of proteins [Z. Zhang and D. L. Smith, *Protein Sci* **2**, 522 (1993)].
25. We thank Brian Green at VG Biotech for helpful discussions. The Oxford Centre for Molecular Sciences is supported by the UK Science and Engineering Research Council; and Medical Research Council. Supported in part by an International Research Scholars Award (C.M.D.) from the Howard Hughes Medical Institute. S.E.R. is a Royal Society 1983 University Research Fellow.

12 April 1993; accepted 14 July 1993

Determination of Type I Receptor Specificity by the Type II Receptors for TGF-β or Activin

Reinhard Ebner, Ruey-Hwa Chen, Sean Lawler, Thomas Zioncheck, Rik Derynck*

Transforming growth factor–β (TGF-β) and activin signal primarily through interaction with type I and type II receptors, which are transmembrane serine-threonine kinases. Tsk 7L is a type I receptor for TGF-β and requires coexpression of the type II TGF-β receptor for ligand binding. Tsk 7L also specifically bound activin, when coexpressed with the type IIA activin receptor. Tsk 7L could associate with either type II receptor and the ligand binding specificity of Tsk 7L was conferred by the type II receptor. Tsk 7L can therefore act as type I receptor for both activin and TGF-β, and possibly other ligands.

Peptide growth and differentiation factors exert their effects by interacting with specific cell surface receptors. Several receptors, including the type II activin (*1*) and TGF-β (*2*) receptors and a type I receptor for TGF-β, Tsk 7L (*3*), have been shown to be transmembrane serine-threonine kinases. Within the TGF-β superfamily of growth and differentiation factors (*4*), the receptor-ligand interactions have been best studied for TGF-β and activin. In the case of TGF-β, the type I and type II receptors, defined on the basis of the size of the ^{125}I–TGF-β–cross-linked receptors on polyacrylamide gels, mediate most biological activities of TGF-β (*5*, 6). The type II receptor, possibly in conjunction with the type I receptor, is required for the antiproliferative effect of TGF-β, whereas the type I receptor mediates TGF-β–induced expression of genes involved in cell-matrix interactions (*7*). Cross-linking experiments similarly revealed type II and type I receptors for activin, corresponding in size to the respective TGF-β receptors (*1*, *8*). Ligand competition experiments suggested that activin and TGF-β bind to distinct and specific type II receptors (*1*, *2*). Overexpression of truncated type II receptors for TGF-β (*7*) and activin (*9*) inhibit ligand-induced responses in a dominant negative fashion, suggesting that oligomerization of receptor subunits is critical for function. A direct physical interaction of the TGF-β type I and type II receptors was proposed based on coimmunoprecipitation experiments (6).

After transfection, the type II TGF-β and activin receptors can bind their respective ligands (*1*, *2*). In contrast, Tsk 7L binds TGF-β only when coexpressed with the type II TGF-β receptor (*3*). To further evaluate the ligand specificity of Tsk 7L, we coexpressed Tsk 7L or its truncated form, which is missing most of the cytoplasmic domain (*3*), with the isogenic type IIA activin receptor (*1*) (Fig. 1A, left). In this case, ^{125}I-activin, but not ^{125}I–TGF-β (*10*), bound to both the type II activin receptor and Tsk 7L as shown by cross-linking. Coexpression of truncated Tsk 7L resulted in the appearance of a faster migrating band that was cross-linked to ^{125}I-activin as predicted. Tsk 7L did not bind ligand in the absence of the type II activin receptor. Coexpression of a control transmembrane protein such as TGF-α with the type II activin receptor resulted in binding of ^{125}I-activin only to the type II activin receptor. A chimeric type II receptor, containing the extracellular domain of the activin receptor and the transmembrane and cytoplasmic domains of the TGF-β receptor, by itself bound activin and not TGF-β and also conferred binding of activin and not TGF-β to the truncated Tsk 7L (*11*). Thus, the ligand binding specificity of the type I receptor is determined by the extracellular domain of the coexpressed type II receptor.

When cotransfected with the type II TGF-β receptor, Tsk 7L and its truncated form bound ^{125}I–TGF-β (Fig. 1A, right), as reported (*3*). Thus, Tsk 7L is a type I receptor that can specifically bind TGF-β or activin, depending on the nature of the cotransfected type II receptor. As reported for TGF-β binding to the type II TGF-β receptor (*3*), coexpression of Tsk 7L with the type II activin receptor inhibited binding of ^{125}I-activin to the type II receptor, an effect not readily seen with the truncated Tsk 7L. Most subsequent experiments will be illustrated only with the truncated Tsk 7L, but the truncated and full-size receptor had a similar ability to bind ligand (*10*).

Competition experiments showed that unlabeled activin, but not TGF-β, could displace ^{125}I-activin bound to Tsk 7L in the presence of the type II activin receptor (Fig. 1B, left). Similarly, only TGF-β, but not activin, could displace ^{125}I–TGF-β bound to the type I receptor in the presence of the type II TGF-β receptor (Fig. 1B, right). To compare the relative affinities of activin and TGF-β binding to the type I receptor, the radiolabeled ligands were cross-linked in the presence of increasing concentrations of unlabeled ligands. In the case of both activin and TGF-β, labeled ligand bound to the type I receptor and the type II receptor was displaced at approximately the same concentration (Fig. 1, C and D). The 50% displacement was at 160 to 320 pM for TGF-β, whereas for activin a similar displacement was observed at 800 to 1600 pM of ligand. Thus, the type I receptor bound ligand with a similar apparent affinity as the type II receptor, as observed for endogenous receptors (*5*).

Under certain conditions, the type I TGF-β receptor coimmunoprecipitates with the type II receptor, suggesting a physical interaction between both receptors (6). To evaluate whether the Tsk 7L type I receptor interacts with the type II TGF-β and activin receptors, we coexpressed the full-size or truncated type I receptor containing a COOH-terminal epitope tag with the type II TGF-β or activin receptor lacking this tag. After binding and cross-linking to ^{125}I-labeled ligand, a tag-specific antibody immunoprecipitated the type I receptor and coimmunoprecipitated the type II receptor, suggesting a physical interaction between these two receptor types (Fig. 2A). The intensity of the type II receptor band was frequently less than the type I receptor and was relatively lower in the case of the activin bound type II activin receptor (Fig. 2C, lane 2) than the TGF-β bound type II receptor (Fig. 2B, lane 2). This may be the result of a somewhat weaker interaction of Tsk 7L with the type II activin receptor than with the type II TGF-β recep-

R. Ebner, R.-H. Chen, S. Lawler, R. Derynck, Departments of Growth and Development, and Anatomy, Programs in Cell Biology and Developmental Biology, University of California at San Francisco, San Francisco, CA 94143–0640.
T. Zioncheck, Department of Protein Chemistry, Genentech, South San Francisco, CA 94080.

*To whom correspondence should be addressed.